

## NANOG improves type I collagen expression in human fetal scleral fibroblasts

Xuyan Li<sup>1,2</sup>, Tianfei Yu<sup>1,2</sup>, Ming Li<sup>2</sup>, Youqi Wang<sup>2</sup>, Bo Meng<sup>2</sup> and Yanshuang Mu<sup>1,\*</sup>

<sup>1</sup> Key Laboratory of Animal Cellular and Genetic Engineering of Heilongjiang Province, Northeast Agricultural University, Harbin, China 150030

<sup>2</sup> College of Life Science and Agriculture Forestry, Qiqihar University, Qiqihar, China 161006

\*Corresponding author: [muyanshuang@neau.edu.cn](mailto:muyanshuang@neau.edu.cn)

Received: July 11, 2018; Revised: September 15, 2018; Accepted: October 11, 2018; Published online: October 23, 2018

**Abstract:** Human fetal scleral fibroblasts (HFSFs) are components of the sclera and play important roles in its structure and function. In myopia, scleral remodeling reduces collagen fibers and the sclera begins to thin. NANOG is a key transcription factor essential for pluripotent and self-renewing phenotypes of undifferentiated embryonic stem cells. To determine whether NANOG improves human fetal scleral fibroblast quality and the underlying mechanisms in these cells, we established stable NANOG-overexpressing HFSFs. We studied type I collagen (*COL1A1*) and Rho-associated coiled-coil protein kinase 1 (*ROCK1*) expression in transfected cells. We also investigated *POU5F1*, *SOX2*, *KLF4*, *MYC* and *SALL4* expression in NANOG stably-overexpressed fibroblasts. Our data show that NANOG expression increased proliferation rates in fibroblasts. When compared to controls, expression of *COL1A1* in transfected fibroblasts was increased and the expression of *ROCK1* was decreased. Similarly, the expression of *POU5F1*, *SOX2* and *KLF4* was downregulated, the expression of *MYC* was upregulated and there was no significant change in the expression of *SALL4* in transfected fibroblasts. Our results suggest that in fibroblasts, NANOG regulates *ROCK1* expression and improves *COL1A1* expression to delay scleral remodeling.

**Keywords:** NANOG, human fetal scleral fibroblasts, myopia, collagen

### INTRODUCTION

Myopia is the most common eye disease in humans [1]. The human sclera, which is formed by fibroblasts and the collagen fiber sheath, is intimately involved in eye growth regulation and the scleral remodeling of myopia formation. In human sclera, the content of type I collagen fibrils is 50-70% of the total collagen fibers, which are mostly distributed along the equator and posterior pole regions of the eyeball [2]. During scleral remodeling in myopia, the posterior sclera becomes thinner and the diameter of collagen fibrils smaller compared to the sclera in normal eyes [3,4]. Scleral fibroblasts, which synthesize and secrete collagen fibrils and matrices, monitor changes in the surrounding extracellular matrix to maintain a balance of synthesis and degradation [5,6]. If scleral fibroblasts decrease proteoglycan synthesis, the biomechanics of the sclera are affected and elongation of the eye is induced [7]. Scleral remodeling and axial length extension can induce refractive errors, retinal degeneration and/or detachment [8,9].

NANOG is essential for transforming dedifferentiated intermediate cells to ground state pluripotency cells in reprogramming processes [10]. *Nanog* overexpression in embryonic stem cells (ESCs) enhances the transfer of pluripotency in fusion experiments and converts epiblast stem cells to ground state pluripotency [11]. *Nanog* is a novel pluripotent gene that plays crucial roles in maintaining the undifferentiated state of mouse embryonic stem cells (mESCs) [12,13]. In generating induced pluripotent stem cells (iPSCs), NANOG participates indirectly in cell reprogramming by interacting with the four pluripotent-associated genes, *POU5F1*, *SOX2*, *KLF4* and *MYC* [14]. It has been shown that NANOG directly participates in reprogramming human somatic cells by combining with *Lin28*, *POU5F1* and *SOX2* [15-17]. The activation of endogenous *Nanog* is essential for generating iPSCs, which can contribute to adult chimeras [18,19]. Ectopic expression of *Nanog* in NIH3T3 cells promotes entry into S phase and increases cellular growth rates [20,21].

In this study, we cloned the full length of the human *NANOG* coding region, constructed the eukaryotic expression vector of *NANOG* and transfected it into HFSFs, where we systematically investigated biological cellular characteristics (proliferation) and assessed *COL1A 1* and *ROCK1* expression in stably-transfected cells. The expression of *POU5F1*, *SOX2*, *NANOG*, *KLF4*, *MYC* and *SALL4* was also assessed. Our objective was to detect the effects of *NANOG* expression on the sclera by evaluating its influence on cell proliferation and *COL1A 1* expression in HFSFs. By determining the underlying mechanisms of *NANOG* expression in these cells, we hoped to clarify the mechanism of myopia formation and provide theoretical support for myopia treatment.

## MATERIALS AND METHODS

### *Gene cloning and vector construction*

The coding sequence of human *NANOG* was PCR-amplified from pPyCAG:h*NANOG* [12] using the following sense 5'-ATGAGTGTGGATCCAGCTTGTC-3' and antisense primers 5'-TCACATATCTTCAGGCTGTATG-3'. The PCR amplification was carried out as follows: one cycle at a denaturing temperature of 94°C for 4 min, and 35 subsequent cycles; denaturation at 95°C for 30 s, annealing at 56.5°C for 30 s, extension at 72°C for 30 s, and a final extension at 72°C for 10 min. To construct a *NANOG* mammalian expression plasmid, the *NANOG* coding sequence was inserted into pcDNA3.1 (+) (Invitrogen, Shanghai, China) between the *Hind* III and *Xho* I restriction enzyme sites to generate pcDNA3.1(t)/*NANOG*. The *NANOG* cDNA was also inserted into pEGFP-C1 (Invitrogen, Shanghai, China) between the *Bgl* II and *Xho* I restriction enzyme sites to generate pEGFP-C1/*NANOG*, which expresses a GFP-*NANOG* fusion protein.

### **Cell culture and transfection**

This study was approved by the Ethics Committee of Harbin Medical University in China. HFSFs were obtained from Beijing Institute of Ophthalmology (Beijing, China) [22],[23]. The fibroblasts were cultured in Dulbecco's modified Eagle's medium (DMEM) (Invitrogen, Shanghai, China) with 1% antibiotic/anti-

mycotic penicillin-streptomycin (Invitrogen, Shanghai, China), 10% fetal bovine serum (FBS), (Invitrogen, Shanghai, China) and incubated at 37°C in a humidified incubator with 5% CO<sub>2</sub>. The growth medium was changed every two days. When the cultures reached 90% confluence, the cells were trypsinized for 1 min at 37°C in 0.25% trypsin/EDTA and subcultured at a ratio of 1:3 (cells to media) in 25 mm<sup>2</sup> plastic cell culture bottles (Invitrogen, Shanghai, China).

The cells were randomized into 4 groups: control-untreated HFSFs group (control), the empty pcDNA3.1 vector-transfected HFSFs group (mock), *NANOG*-transfected HFSFs group (*NANOG*-trans) and GFP-*NANOG*-transfected HFSFs group (GFP-*NANOG*-transfected). For transfection experiments, the cells were plated in 3.5-cm plates (Invitrogen, Shanghai, China) in HFSFs culture medium without penicillin/streptomycin to achieve 70-80% confluence over 24 h. Cells were transfected with lipofectamine 2000 (Invitrogen, Shanghai, China) according to the manufacturer's instructions at a ratio of 3:1 (transfection reagent (mL):DNA (mg)). Cells were passaged 24 h after transfection. The flasks were then supplemented with DMEM selection medium (high glucose supplemented with 10% FBS and 400 ng/mL G418), after cell adhesion. Cells for stable selection were rendered by G418 selection for 14 days until all untransfected cells died. For the pcDNA3.1 (t)/*NANOG* plasmid and pEGFP-C1/*NANOG* plasmid transfections, all growth and selection conditions were identical.

### **Cell growth curve and cell viability**

For the cell growth curve, cells were seeded at 1x10<sup>4</sup> cells/dish in 35-mm dishes (Invitrogen, Shanghai, China) in DMEM supplemented with 10% FBS. Cell numbers were determined using a hemocytometer. The cell growth curve was drawn according the cell number. Cell viability was determined by the trypan blue exclusion assay. Trypan blue at a concentration of 0.5% was mixed with equal volumes of cell suspensions in DMEM and 10% FBS. Cells excluding the dye were also determined. Both cell counts and the trypan blue exclusion assays were performed in triplicate, with standard deviations (SD) for each time point.

## RNA isolation, reverse transcription and real time PCR

HFSFs cells were seeded in 25-mm<sup>2</sup> plastic bottles at  $5 \times 10^5$  cells/mL. After culturing for 24 h, the cells were harvested for total RNA extraction using Trizol Reagent (Invitrogen, Shanghai, China). Complementary DNA (cDNA) was synthesized according to the manufacturer's instructions (Fermentas, Shanghai, China), generating about 4 µg of total RNA. Based on sequences from the GenBank database (Supplementary Table S1), *COL1A1*, *ROCK1*, *NANOG*, *POU5F1*, *SOX2*, *KLF4*, *MYC*, *SALL4*, *ACTB* and *GAPDH* primers were designed using Primer-Premier 5 (Premier Biosoft Interpairs, CA, USA).

End-point PCR was performed on a Biometra PCR System (Biometra, Munchen, DE). A typical reaction was performed in 25 µL; it consisted of 2 µL cDNA, 12.5 µL 2×ExTaq PCR Master Mix buffer (TaKaRa, Dalian, China) and primer pairs (10 pmol each). An initial PCR temperature cycle was performed for 4 min at 95°C, followed by 28 cycles of primer annealing for 30 s at 59°C, and extension for 30 s at 72°C. Negative controls for end-point PCR contained no template. The PCR products were examined by 1% agarose gel electrophoresis (TaKaRa, Dalian, China) in TAE buffer at 11 V/cm for 30 min.

Quantitative real-time PCR (qPCR) was performed on an ABI7500 Fast Real-Time PCR System (Applied Biosystems, CA, USA). A typical reaction was performed in 25 µL; it consisted of 2 µL cDNA, 12.5 µL 2×SYBR Green PCR buffer and primer pairs (10 pmol each). An initial PCR temperature cycle was performed for 2 min at 95°C, followed by 40 cycles of primer annealing for 30 s at 60°C, and extension for 30 s at 72°C. Negative controls for the qPCR contained no template. The change in threshold cycle ( $\Delta Ct$ ) was calculated by subtracting the average Ct of GAPDH mRNA from the average Ct of target genes. NANOG-trans and mock samples were normalized to the control, and the t-test was performed on NANOG-trans versus mock groups. All experiments were performed in triplicate. Comparative quantification values were obtained from the Ct number, where an increase in signal was associated with an exponential increase in PCR products.

## Hoechst 33342 staining and fluorescence microscopy

After transfection with the plasmid encoding EGFP-NANOG, the HFSFs were stained using Hoechst 33342 (Sigma, Shenyang, China). Cells were washed three times in Dulbecco's phosphate-buffered saline (DPBS) and fixed in 4% (w/v) paraformaldehyde/4% (w/v) sucrose in DPBS for 40 min at room temperature. The HFSFs were then stained with 5 mg/mL Hoechst 33342 for 8 min and washed twice in DPBS. Cells were placed on a glass slide, and Antifade mounting medium (Abcam, Beijing, China) was added and sealed with nail polish. Samples were assessed by fluorescence microscopy at 530 nm and 480 nm excitation wavelengths (Olympus BX51, Japan).

## Western blotting

Total cellular protein was extracted from HFSFs by lysing cells in ice-cold radioimmunoprecipitation assay buffer containing protease inhibitors, 50 mM Tris-HCl, pH 8.0, 150 mM NaCl, 1% NP-40, at 4°C and phosphatase inhibitors (R&D Systems, Shanghai, China). After centrifugation at  $12000 \times g$  (30 min at 4°C), the supernatants were collected and protein concentrations measured using the bicinchoninic acid (BCA) Protein Assay kit (Beyotime, Beijing, China). Samples containing 50 µg of protein were mixed with loading dye and were subjected to sodium dodecyl sulfate polyacrylamide gel electrophoresis (SDS-PAGE) in 12% polyacrylamide gels, and transferred onto polyvinylidene difluoride membranes (Millipore, MA, USA). The membranes were blocked in 5% Tris-buffered saline (10 mM Tris-HCl, pH 8.0, 150 mM NaCl, 0.5% Tween-20 and 5% fat-free dry milk) for 1 h at room temperature. The membranes were then probed overnight at 4°C with specific primary antibodies against type I collagen (1:1000) (Abcam, CA, USA), ROCK1 (1:1000) (CST, CA, USA) and ACTB (1:1000) (Sigma, Shenyang, China), which acted as a loading control. The following day, the membranes were washed and incubated with a horseradish peroxidase (HRP)-conjugated anti-rabbit goat IgG antibody (1:1000) (Abmart, Beijing, China). The membranes were developed using an enhanced chemiluminescence (ECL) kit (Thermo Fisher Scientific, Shanghai, China), according to the manufacturer's instructions. Band

intensity was quantified by densitometry using ImageJ software (version 1.38). The relative level of protein expression was expressed as the density ratio of the protein compared to ACTB levels in the same sample.

### Statistical analysis

Statistical analyses were performed using SPSS 16.0 Statistical Software (SPSS, Inc., Chicago, IL, USA). All data were expressed as the mean $\pm$ SD of at least three separate repeated experiments. The differences between exposed and untreated cells were analyzed by t-test. Values of  $p < 0.05$  were considered statistically significant.

## RESULTS

### Expression of human NANOG in HFSFs

Two eukaryotic expression vectors were constructed to express human NANOG and GFP-NANOG fusion proteins, respectively (Fig. 1A). RT-qPCR results demonstrated that NANOG mRNA was successfully expressed in NANOG stably-transfected HFSFs (Fig. 1B). Western blot analysis also showed that NANOG was expressed in HFSFs, which were stably transfected by pcDNA3.1 (t)/NANOG (Fig. 1C).

### Ectopically expressed NANOG localizes to the nucleus and promotes HFSFs cell growth

We measured the effects of NANOG expression on HFSFs cell growth. NANOG transfected HFSFs showed an increased proliferation rate compared to those of the mock HFSFs ( $P < 0.05$ ), while the rate of cell growth was similar between the mock and control HFSFs ( $P > 0.05$ ) (Fig. 2A).

In ESCs, NANOG contains a homeodomain, suggesting it acts as a transcriptional regulator and should localize to the nucleus [11,24]. To verify the subcellular localization of ectopically-expressed NANOG, we generated a construct comprising NANOG fused to Enhanced Green Fluorescent Protein (EGFP-NANOG). The results showed that EGFP-NANOG was localized to the nucleus in HFSFs (Fig. 2D). This observation suggests that NANOG encodes a nuclear localization signal and regulates gene transcription in nucleus [25].

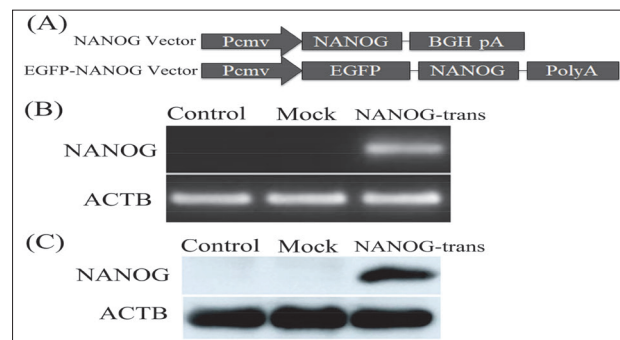


**Fig. 1.** Expression of human NANOG in HFSFs. **A** – NANOG plasmid (GFP and pcDNA3.1) construction. **B** – NANOG expression in HFSFs was detected by end-point PCR. ACTB acted as a loading control. Control – the control-untreated HFSFs. Mock – the empty pcDNA3.1 vector-transfected HFSFs. NANOG-trans – NANOG-transfected HFSFs. **C** – NANOG protein expression levels were determined by Western blotting. Equal protein concentrations were loaded in each lane. ACTB acted as a loading control. Control – the control-untreated HFSFs. Mock – the empty pcDNA3.1 vector-transfected HFSFs. NANOG-trans – NANOG-transfected HFSFs.

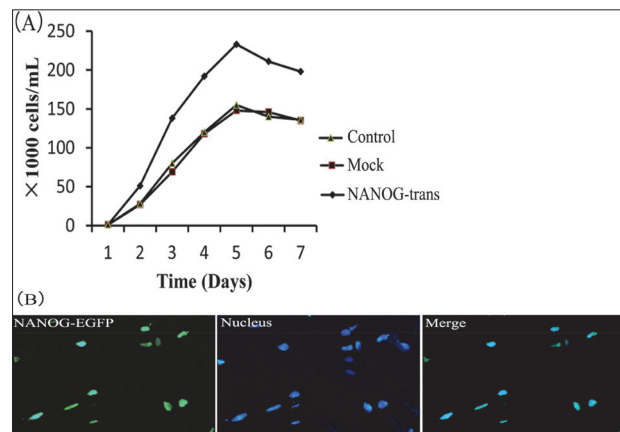


**Fig. 2.** NANOG gene expression promoted cell growth and nuclear localization of NANOG-EGFP. **A** – Proliferation of HFSFs. Control – the control-untreated HFSFs. Mock – the empty pcDNA3.1 vector-transfected HFSFs. NANOG-trans – NANOG-transfected HFSFs. **B** – Localization of NANOG-EGFP in HFSFs. NANOG-EGFP – GFP-NANOG-transfected HFSFs. Nucleus – Hoechst 33342 staining of the HFSFs cell nucleus. Merged image of NANOG-EGFP and Nucleus.

### NANOG affects COL1A1 and ROCK1 expression in HFSFs

NANOG expression significantly increased COL1A1 mRNA expression in NANOG-trans HFSFs compared to the mock HFSFs ( $P < 0.05$ ), while for expression of COL1A1 mRNA, there were no significant differences between mock and control HFSFs ( $P > 0.05$ ).

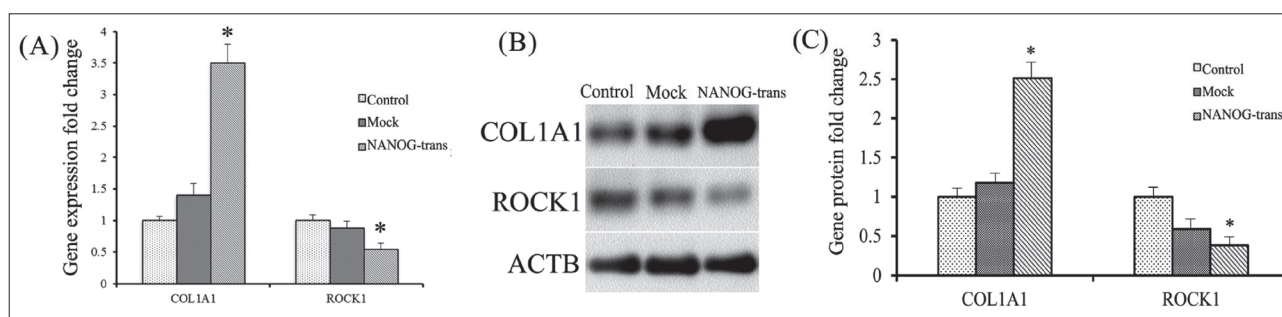


**Fig. 3.** *NANOG* affects *COL1A1* and *ROCK1* expression in HFSFs. **A** – *NANOG* affects *COL1A1* and *ROCK1* mRNA expression. Fold difference was calculated with respect to the control-untreated HFSFs and the HFSFs transfected with pcDNA3.1 empty vector. Control – the control-untreated HFSFs. Mock – the empty pcDNA3.1 vector-transfected HFSFs. *NANOG*-trans – *NANOG*-transfected HFSFs. Bars represent the mean±standard errors of three independent experiments. *NANOG*-trans and mock were normalized to the control and statistical analysis was performed on *NANOG*-trans vs mock. **B** – *COL1A1* and *ROCK1* protein expression levels were determined by Western blotting. Control – the control-untreated HFSFs. Mock – the empty pcDNA3.1 vector-transfected HFSFs. *NANOG*-trans – *NANOG*-transfected HFSFs. **C** – Corresponding densitometric analyses of the protein bands of *COL1A1* and *ROCK1* protein. Control – the control-untreated HFSFs. Mock – the empty pcDNA3.1 vector-transfected HFSFs. *NANOG*-trans – *NANOG*-transfected HFSFs. *NANOG*-trans and mock were normalized to the control, and statistical analysis was performed on *NANOG*-trans versus mock. \* $P < 0.05$  indicates significant differences.

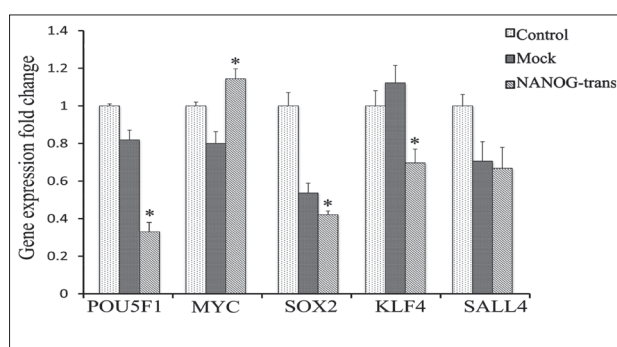


**Fig. 4.** Relative expression of pluripotent-related genes after stable transfection by pcDNA3.1-*NANOG* in HFSFs. Fold difference was calculated with respect to the control-untreated HFSFs and the HFSFs transfected with pcDNA3.1 empty vector. Control – the control-untreated HFSFs. Mock – the empty pcDNA3.1 vector-transfected HFSFs. *NANOG*-trans – *NANOG*-transfected HFSFs. Bars represent the mean±standard errors of three independent experiments. *NANOG*-trans and mock were normalized to the control, and statistical analysis was performed on *NANOG*-trans versus mock. \* $P < 0.05$  indicates significant differences.

(Fig.3A). *NANOG* expression significantly increased the *COL1A1* protein level in *NANOG*-trans HFSFs compared to mock HFSFs ( $P < 0.05$ ) (Fig. 3B and C). There were no significant differences in protein levels between the mock and control HFSFs ( $P > 0.05$ ) (Fig. 3B and C). *ROCK1* mRNA levels were decreased in *NANOG*-trans HFSFs as compared to mock HFSFs ( $P < 0.05$ ) (Fig.3A). Reduced *ROCK1* protein levels also correlated with decreased mRNA levels in *NANOG*-

trans HFSFs compared to the mock HFSFs ( $P < 0.05$ ) (Fig. 3B and C). These data suggest that *COL1A1* and *ROCK1* expression in HFSFs was significantly affected by *NANOG* expression.

#### Activation of pluripotent genes by *NANOG* overexpression in HFSFs

To clarify whether *NANOG* interacted with other key pluripotent genes thereby increasing *COL1A1* expression in HFSFs, we investigated the expression levels of pluripotent genes including *POU5F1*, *SOX2*, *KLF4*, *MYC* and *SALL4* in *NANOG* stably-transfected HFSFs, using qPCR (Fig. 4). Compared with the mock HFSFs, the expression of *POU5F1*, *SOX2* and *KLF4* significantly declined in *NANOG*-trans HFSFs ( $p < 0.05$ ). The expression of *MYC* significantly increased in *NANOG*-trans HFSFs compared to the mock HFSFs ( $p < 0.05$ ). There was no significant change in *SALL4* in *NANOG*-trans HFSFs compared to the mock HFSFs ( $p > 0.05$ ).

#### DISCUSSION

The development of myopia in humans is associated with marked thinning of the sclera, the tough outer coat of the eye that facilitates change in eye size [4]. This altered scleral morphology is associated with local changes in collagen fibril ultrastructure and

increased numbers of small-diameter collagen fibrils [26]. In addition, there is a more lamellar organization of posterior scleral collagen fibril bundles [27]. Scleral fibroblasts, which synthesize and secrete the collagen fibrils, are involved in scleral remodeling and play important roles in the control of eye size and myopia development [28,29]. In a previous study, the overexpression of *NANOG* in mouse fibroblasts promoted cell entry into the S phase and cell proliferation [20]. Our results show that constitutive overexpression of *NANOG* significantly increased HFSFs proliferation. *NANOG*, through CDK6 and CDC25A binding, allows human ESCs to enter the S phase from the G1 phase [30]. Compared with normal ESCs, the ESCs with a higher expression level of CDK6 and CDC25A in the S phase had a shorter cycle time to enter the next S phase [30]. In murine NIH3T3 cells, cell proliferation was accelerated when *Nanog* was highly expressed [20,31], therefore reducing *NANOG* expression could reduce breast cancer cell proliferation [32]. From these observations, it appears that *NANOG* plays an important role in regulating HFSFs proliferation.

Collagen accounts for 90% of scleral dry weight, the majority of this being type I collagen [33]. As the main component of the sclera, type I collagen is involved in connective tissue growth and extracellular matrix reorganization [2]. The *COL1A1* gene produces the pro- $\alpha$ 1 chain, which combines with another pro- $\alpha$ 1 chain and also with a pro- $\alpha$ 2 chain (produced by the *COL1A2* gene) to create a molecule of type I procollagen [34]. It has been reported that a *COL1A1* polymorphism was statistically associated with simple myopia phenotypes [35,36]. Similarly, *COL1A1* reductions appear to trigger scleral remodeling and induce myopia [3]. Our results demonstrated that *NANOG* upregulated *COL1A1* mRNA and protein expression in HFSFs, indicating that *NANOG* increases collagen synthesis in the sclera and may delay sclera remodeling, which is a potential risk factor for eye elongation.

The small molecule Rho GTP enzyme family has regulatory roles in fibroblast cytoskeleton rearrangement, cell proliferation and gene transcription [37]. *ROCK1* is an extremely important downstream protein in the Rho signaling pathway [37]. When extracellular stimuli activate G-protein-coupled receptors, Rho proteins are activated and combine with ROCK to induce

downstream biological effects, such as cytoskeletal reorganization and fiber synthesis of fibroblasts [38]. Activation of the Rho A/ROCK1 signaling pathway upregulates *COL1A1* expression at the extracellular matrix (ECM); however, this reaction can be altered by using the inhibitor Y-27632, which inhibits *ROCK1* expression, blocking the RhoA/ROCK1 signaling pathway and thereby downregulating *COL1A1* expression at the ECM [39]. By contrast, in this study, *ROCK1* expression decreased after *NANOG* overexpression in HFSFs, suggesting that *NANOG* may improve *COL1A1* synthesis by activating other signaling pathways.

In ESCs, *NANOG*, *POU5F1*, *SOX2* and *KLF4* were the core pluripotency transcription factors maintaining the pluripotent state of these cells [40]. *POU5F1*, *SOX2* and *NANOG* function together to form a regulatory loop to maintain ES cell pluripotency and self-renewal [24]. *KLF4* is upstream of *NANOG* and cooperates with *PBX1* directly to regulate *NANOG* expression in human ESCs [41]. To determine whether *NANOG* regulates the cell cycle, *COL1A1* and *ROCK1* expression through other pluripotency-related genes in HFSFs, we examined the expression of *POU5F1*, *SOX2* and *KLF4*. Our results demonstrated that although *NANOG* was maintained at the 20-fold higher level than normal HFSFs, the expression of *POU5F1*, *SOX2* and *KLF4* was downregulated. These results showed that only *NANOG* overexpression cannot reactivate the expression of pluripotency-related genes in HFSFs. *Sall4* is an important component of the transcription regulatory networks in ESCs and cooperates with *NANOG* [42]. In this study, *SALL4* expression remained unchanged after *NANOG* overexpression. This is because *SALL4* activation by *NANOG* requires *POU5F1* and *SOX2* participation. *MYC* is an important cell-cycle regulator and promotes cell proliferation [43]. In a previous study, it was shown that *NANOG* binds on the *MYC* promoter region to promote expression [32]. In the present study, *MYC* expression was significantly increased after *NANOG* overexpression; therefore, *MYC* may be the main factor in promoting HFSF proliferation.

## CONCLUSION

The present study shows that the expression of *NANOG* increased HFSF proliferation and improved *COL1A1* synthesis in HFSFs. However, the molecular mecha-

nisms underlying *NANOG* gene function in HFSFs is not yet clear. Additional studies will be required to clarify the precise mechanism by which *NANOG* participates in regulating collagen synthesis in HFSFs.

**Acknowledgment:** This work was supported by the Open Projects of Key Laboratory of Animal Cellular and Genetic Engineering of Heilongjiang Province (KF201709).

**Author contributions:** Yanshuang Mu, designed the study, conducted the experimental work, analyzed the results and wrote the first draft of the manuscript. Xuyan Li, Tianfei Yu, Ming Li and Youqi Wang participated in designing the study, the experimental work, and in obtaining and analyzing the results. Bo Meng participated in drafting the article and critically revising it. All authors contributed to and have approved the final manuscript.

**Conflict of interest disclosure:** The authors have no financial interests or potential conflicts of interests to declare.

## REFERENCES

- Holden B, Sankaridurg P, Smith E, Aller T, Jong M, He M. Myopia, an underrated global challenge to vision: where the current data takes us on myopia control. *Eye (Lond)*. 2014;28:142-6.
- Watson PG, Young RD. Scleral structure, organisation and disease. A review. *Exp Eye Res*. 2004;78:609-23.
- McBrien NA, Cornell LM, Gentle A. Structural and ultra-structural changes to the sclera in a mammalian model of high myopia. *Invest Ophthalmol Vis Sci*. 2001;42:2179-87.
- Gentle A, Liu Y, Martin JE, Conti GL, McBrien NA. Collagen gene expression and the altered accumulation of scleral collagen during the development of high myopia. *J Biol Chem*. 2003;278:16587-94.
- McBrien NA, Gentle A. Role of the sclera in the development and pathological complications of myopia. *Prog Retin Eye Res*. 2003;22:307-38.
- Hu S, Cui D, Yang X, Hu J, Wan W, Zeng J. The crucial role of collagen-binding integrins in maintaining the mechanical properties of human scleral fibroblasts-seeded collagen matrix. *Mol Vis*. 2011;17:1334-42.
- Rada JA, Nickla DL, Troilo D. Decreased proteoglycan synthesis associated with form deprivation myopia in mature primate eyes. *Invest Ophthalmol Vis Sci*. 2000;41:2050-8.
- Rada JA, Johnson JM, Achen VR, Rada KG. Inhibition of scleral proteoglycan synthesis blocks deprivation-induced axial elongation in chicks. *Exp Eye Res*. 2002;74:205-15.
- Cui W, Bryant MR, Sweet PM, McDonnell PJ. Changes in gene expression in response to mechanical strain in human scleral fibroblasts. *Exp Eye Res*. 2004;78:275-84.
- Silva J, Chambers I, Pollard S, Smith A. Nanog promotes transfer of pluripotency after cell fusion. *Nature*. 2006;441:997-1001.
- Silva J, Nichols J, Theunissen TW, Guo G, van Oosten AL, Barrandon O, Wray J, Yamanaka S, Chambers I, Smith A. Nanog is the gateway to the pluripotent ground state. *Cell*. 2009;138:722-37.
- Chambers I, Colby D, Robertson M, Nichols J, Lee S, Tweedie S, Smith A. Functional expression cloning of Nanog, a pluripotency sustaining factor in embryonic stem cells. *Cell*. 2003;113:643-55.
- Mitsui K, Tokuzawa Y, Itoh H, Segawa K, Murakami M, Takahashi K, Maruyama M, Maeda M, Yamanaka S. The homeoprotein Nanog is required for maintenance of pluripotency in mouse epiblast and ES cells. *Cell*. 2003;113:631-42.
- Miyazari Y, Torres-Padilla ME. Control of ground-state pluripotency by allelic regulation of Nanog. *Nature*. 2012;483:470-3.
- Yu J, Vodyanik MA, Smuga-Otto K, Antosiewicz-Bourget J, Frane JL, Tian S, Nie J, Jonsdottir GA, Ruotti V, Stewart R, Slukvin II, Thomson JA. Induced pluripotent stem cell lines derived from human somatic cells. *Science*. 2007;318:1917-20.
- Choi KD, Yu J, Smuga-Otto K, Salvaggio G, Rehrauer W, Vodyanik M, Thomson J, Slukvin I. Hematopoietic and endothelial differentiation of human induced pluripotent stem cells. *Stem Cells*. 2009;27:559-67.
- Hanna J, Saha K, Pando B, van Zon J, Lengner CJ, Creighton MP, van Oudenaarden A, Jaenisch R. Direct cell reprogramming is a stochastic process amenable to acceleration. *Nature*. 2009;462:595-601.
- Takahashi K, Yamanaka S. Induction of pluripotent stem cells from mouse embryonic and adult fibroblast cultures by defined factors. *Cell*. 2006;126:663-76.
- Okita K, Ichisaka T, Yamanaka S. Generation of germ-line-competent induced pluripotent stem cells. *Nature*. 2007;448:313-7.
- Zhang J, Wang X, Chen B, Suo G, Zhao Y, Duan Z, Dai J. Expression of Nanog gene promotes NIH3T3 cell proliferation. *Biochem Biophys Res Commun*. 2005;338:1098-102.
- Piestun D, Kochupurakkal BS, Jacob-Hirsch J, Zeligson S, Koudritsky M, Domany E, Amarglio N, Rechavi G, Givol D. Nanog transforms NIH3T3 cells and targets cell-type restricted genes. *Biochem Biophys Res Commun*. 2006;343:279-85.
- Huo L, Cui D, Yang X, Gao Z, Trier K, Zeng J. All-trans retinoic acid modulates mitogen-activated protein kinase pathway activation in human scleral fibroblasts through retinoic acid receptor beta. *Mol Vis*. 2013;19:1795-803.
- Cui D, Trier K, Chen X, Zeng J, Yang X, Hu J, Ge J. Distribution of adenosine receptors in human sclera fibroblasts. *Mol Vis*. 2008;14:523-9.
- Boyer LA, Lee TI, Cole MF, Johnstone SE, Levine SS, Zucker JP, Guenther MG, Kumar RM, Murray HL, Jenner RG, Gifford DK, Melton DA, Jaenisch R, Young RA. Core transcriptional regulatory circuitry in human embryonic stem cells. *Cell*. 2005;122:947-56.
- Do HJ, Lim HY, Kim JH, Song H, Chung HM, Kim JH. An intact homeobox domain is required for complete nuclear localization of human Nanog. *Biochem Biophys Res Commun*. 2007;353:770-5.
- Curtin BJ, Teng CC. Scleral changes in pathological myopia. *Trans Am Acad Ophthalmol Otolaryngol*. 1958;62:777-88;discussion 88-90.

27. Curtin BJ, Iwamoto T, Renaldo DP. Normal and staphylomatous sclera of high myopia. An electron microscopic study. *Arch Ophthalmol*. 1979;97:912-5.
28. Seyhan N, Canseven AG. In vivo effects of ELF MFs on collagen synthesis, free radical processes, natural antioxidant system, respiratory burst system, immune system activities, and electrolytes in the skin, plasma, spleen, lung, kidney, and brain tissues. *Electromagn Biol Med*. 2006;25:291-305.
29. Nakajima H, Kishi T, Tsuchiya Y, Yamada H, Tajima S. Exposure of fibroblasts derived from keloid patients to low-energy electromagnetic fields: preferential inhibition of cell proliferation, collagen synthesis, and transforming growth factor beta expression in keloid fibroblasts in vitro. *Ann Plast Surg*. 1997;39:536-41.
30. Zhang X, Neganova I, Przyborski S, Yang C, Cooke M, Atkinson SP, Anyfantis G, Fenyk S, Keith WN, Hoare SF, Hughes O, Strachan T, Stojkovic M, Hinds PW, Armstrong L, Lako M. A role for NANOG in G1 to S transition in human embryonic stem cells through direct binding of CDK6 and CDC25A. *J Cell Biol*. 2009;184:67-82.
31. Jeter CR, Liu B, Liu X, Chen X, Liu C, Calhoun-Davis T, Repass J, Zaehres H, Shen JJ, Tang DG. NANOG promotes cancer stem cell characteristics and prostate cancer resistance to androgen deprivation. *Oncogene*. 2011;30:3833-45.
32. Han J, Zhang F, Yu M, Zhao P, Ji W, Zhang H, Wu B, Wang Y, Niu R. RNA interference-mediated silencing of NANOG reduces cell proliferation and induces G0/G1 cell cycle arrest in breast cancer cells. *Cancer Lett*. 2012;321:80-8.
33. Jobling AI, Gentle A, Metlapally R, McGowan BJ, McBrien NA. Regulation of scleral cell contraction by transforming growth factor-beta and stress: competing roles in myopic eye growth. *J Biol Chem*. 2009;284:2072-9.
34. Wessel H, Anderson S, Fite D, Halvas E, Hempel J, Sundar-Raj N. Type XII collagen contributes to diversities in human corneal and limbal extracellular matrices. *Invest Ophthalmol Vis Sci*. 1997;38:2408-22.
35. Metlapally R, Li YJ, Tran-Viet KN, Abbott D, Czaja GR, Malecaze F, Calvas P, Mackey D, Rosenberg T, Paget S, Zayats T, Owen MJ, Guggenheim JA, Young TL. COL1A1 and COL2A1 genes and myopia susceptibility: evidence of association and suggestive linkage to the COL2A1 locus. *Invest Ophthalmol Vis Sci*. 2009;50:4080-6.
36. Nakanishi H, Yamada R, Gotoh N, Hayashi H, Yamashiro K, Shimada N, Ohno-Matsui K, Mochizuki M, Saito M, Iida T, Matsuo K, Tajima K, Yoshimura N, Matsuda F. A genome-wide association analysis identified a novel susceptible locus for pathological myopia at 11q24.1. *PLoS Genet*. 2009;5:e1000660.
37. Nakayamada S, Kurose H, Saito K, Mogami A, Tanaka Y. Small GTP-binding protein Rho-mediated signaling promotes proliferation of rheumatoid synovial fibroblasts. *Arthritis Res Ther*. 2005;7:R476-84.
38. Ridley AJ. Rho family proteins: coordinating cell responses. *Trends Cell Biol*. 2001;11:471-7.
39. Zhu J, Nguyen D, Ouyang H, Zhang XH, Chen XM, Zhang K. Inhibition of RhoA/Rho-kinase pathway suppresses the expression of extracellular matrix induced by CTGF or TGF-beta in ARPE-19. *Int J Ophthalmol*. 2013;6:8-14.
40. Huang CE, Hu FW, Yu CH, Tsai LL, Lee TH, Chou MY, Yu CC. Concurrent expression of Oct4 and Nanog maintains mesenchymal stem-like property of human dental pulp cells. *Int J Mol Sci*. 2014;15:18623-39.
41. Chan KK, Zhang J, Chia NY, Chan YS, Sim HS, Tan KS, Oh SK, Ng HH, Choo AB. KLF4 and PBX1 directly regulate NANOG expression in human embryonic stem cells. *Stem Cells*. 2009;27:2114-25.
42. Wu Q, Chen X, Zhang J, Loh YH, Low TY, Zhang W, Zhang W, Sze SK, Lim B, Ng HH. Sall4 interacts with Nanog and co-occupies Nanog genomic sites in embryonic stem cells. *J Biol Chem*. 2006;281:24090-4.
43. Bretones G, Delgado MD, Leon J. Myc and cell cycle control. *Biochim Biophys Acta*. 2015;1849:506-16.

## Supplementary Data

### Supplementary Table S1.

Available at: [http://serbiosoc.org.rs/NewUploads/Uploads/Li%20et%20al\\_3187\\_Supplementary%20Table%20S1.pdf](http://serbiosoc.org.rs/NewUploads/Uploads/Li%20et%20al_3187_Supplementary%20Table%20S1.pdf)